AD-A036 282 CALIFORNIA INST OF TECH PASADENA DIV OF CHEMISTRY A--ETC F/G 20/8
A SIMPLE SINGLE-COIL DOUBLE RESONANCE NMR PROBE FOR SOLID STATE--ETC(U)
FEB 77 M E STOLL, A J VEGA, R W VAUGHAN N00014-75-C-0960
UNCLASSIFIED TR-5 NL

| OF |
AD
A036282

END

DATE
FILMED
3-77

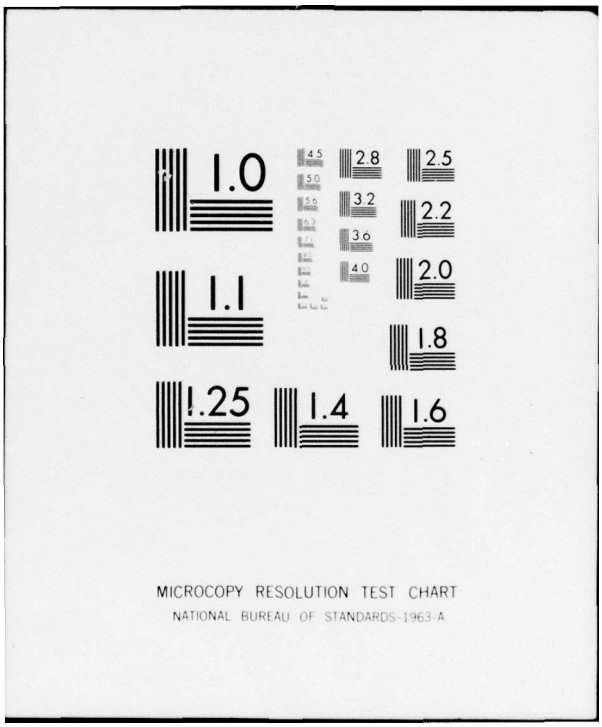
1.0
1.1
1.25
1.4
1.6
1.8
2.0
2.2
2.5
2.8
3.2
3.6
4.0
4.5
5.0
5.6
6.3
7.1
8.0
9.0
MICROCOPY RESOLUTION TEST CHART
NATIONAL BUREAU OF STANDARDS-1963-A

unclassified

SECURITY CLASSIFICATION OF THIS PAGE (When Data Entered)

AD A036282

REPORT DOCUMENTATION PAGE

READ INSTRUCTIONS BEFORE COMPLETING FORM

1. REPORT NUMBER: Technical Report #5	2. GOVT ACCESSION NO.
3. RECIPIENT'S CATALOG NUMBER: Technical report
4. TITLE (and Subtitle): A SIMPLE SINGLE-COIL DOUBLE RESONANCE NMR PROBE FOR SOLID STATE STUDIES	5. TYPE OF REPORT & PERIOD COVERED: interim, Technical Report #5
	6. PERFORMING ORG. REPORT NUMBER
7. AUTHOR(s): M. E. Stoll, A. J. Vega, and R. W. Vaughan	8. CONTRACT OR GRANT NUMBER(s): N00014-75-C-0960
9. PERFORMING ORGANIZATION NAME AND ADDRESS: Division of Chemistry & Chemical Engineering, California Institute of Technology, Pasadena, California 91125	10. PROGRAM ELEMENT, PROJECT, TASK AREA & WORK UNIT NUMBERS: NR-056-605
11. CONTROLLING OFFICE NAME AND ADDRESS: ONR Branch Office ATTN: Dr. R. J. Marcus, 1030 East Green Street, Pasadena, California 91106	12. REPORT DATE: 2/77
	13. NUMBER OF PAGES: 17
14. MONITORING AGENCY NAME & ADDRESS (if different from Controlling Office): 18 p.	15. SECURITY CLASS. (of this report): unclassified
	15a. DECLASSIFICATION DOWNGRADING SCHEDULE

16. DISTRIBUTION STATEMENT (of this Report)

Approved for public release; distribution unlimited

17. DISTRIBUTION STATEMENT (of the abstract entered in Block 20, if different from Report)

TR-5

18. SUPPLEMENTARY NOTES

Submitted for publication

19. KEY WORDS (Continue on reverse side if necessary and identify by block number)

Double resonance, nuclear magnetic resonance, high resolution solid state NMR

20. ABSTRACT (Continue on reverse side if necessary and identify by block number)

A single coil (solenoid), nuclear magnetic double resonance sample probe, suited for a wide variety of solid state studies, is described. It was designed to be used in double resonance experiments where it is necessary to generate intense rf magnetic fields (rotating components with amplitudes about ≈50 gauss) at two widely spaced frequencies and to simultaneously detect microvolt-level signals. Designs for operation over the 12-270 MHz frequency range are discussed.

DD FORM 1 JAN 73 1473 EDITION OF 1 NOV 65 IS OBSOLETE
S/N 0102 LF 014 6601

unclassified
SECURITY CLASSIFICATION OF THIS PAGE (When Data Entered)

071575

A Simple Single-Coil Double Resonance NMR Probe for Solid State Studies

by

M. E. Stoll, A. J. Vega[†], and R. W. Vaughan

Division of Chemistry and Chemical Engineering
California Institute of Technology
Pasadena, California

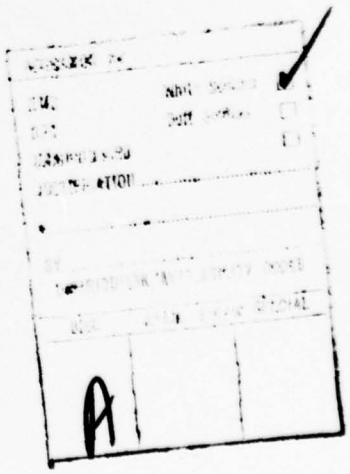

Abstract

A single coil (solenoid), nuclear magnetic double resonance sample probe, suited for a wide variety of solid state studies, is described. It was designed to be used in double resonance experiments where it is necessary to generate intense rf magnetic fields (rotating components with amplitudes ∿50 gauss) at two widely spaced frequencies and to simultaneously detect microvolt-level signals. Designs for operation over the 12-270 MHz frequency range are discussed.

I. Introduction

A critical element of a pulsed nuclear magnetic resonance (NMR) spectrometer suitable for work in solids is the sample probe, a unit designed for application of intense rf magnetic fields to the sample and for detection of the resulting weak rf magnetic fields generated by the sample. This paper will describe a single coil, double resonance sample probe which has been used for a variety of NMR experiments, including both high resolution solid state studies[1,2,3] and liquid studies[4]. These experiments required the generation of rf fields in the sample with rotating components of ∿50 gauss amplitude at two different frequencies simultaneously, as well as the ability to observe weak NMR signals at both frequencies.

Since the probe characteristics often set the practical limitations on the performance of an NMR spectrometer, there have been numerous discussions of probe design in the literature in recent years[5-16], and we will limit our discussion to a presentation of the criteria needed for the recently developed solid state, double resonance experiments[1-3] and a discussion of a particular design we have found convenient and satisfactory over a wide frequency range (from 12-270 MHz). This design is useful when the two rf frequencies are sufficiently separated (a factor of four in our experiments).

II. The Sample Probe

The high resolution, solid state double resonance NMR schemes developed[1-3] require: (a) the generation of rf field strengths of near 50 gauss in the rotating frame at each of two widely separated frequencies, (b) a low degree of rf field inhomogeneity (less than 0.5% over the sample volume) at both frequencies, (c) the spatial pattern of rf field inhomogeneity within the

coil to be identical at both frequencies, (d) and the capability of detecting microvolt-level signals in the solid at each of the rf frequencies while subjecting, or within several microseconds after subjecting, the solid to a high-level (100 watt) irradiation at the second frequency. Essentially, all of these criteria are most easily satisfied by using a single coil for transmitting and receiving both frequencies[5-16], although is does require some electronic means of isolating, or separating, the two frequencies. A single coil configuration is particularly compatible with the restricted space available in the high field magnets.

The design we have found most useful is illustrated in Figure 1. A piece of coaxial cable, one-fourth of a wavelength ($\lambda/4$) at the higher frequency serves a critical isolation role[9,17] by enabling the single coil L to be the inductance in two resonance circuits, each of which can be tuned and impedance matched at its own frequency. It also prevents high-frequency power loss into the low-frequency source while the loss of low-frequency power into the high-frequency source is prevented by keeping C_3 small. This system allows both frequencies to have high Q response and yet furnishes the needed frequency isolation. This scheme has been used over the past two years at a variety of frequencies, and the detailed discussion of the probe circuit will be divided into two sections: one to describe the lower frequency version used for ^{13}C (14.2 MHz) - ^{1}H(56.4 MHz) and ^{207}Pb(12.5 MHz) - ^{19}F(56.4 MHz) double resonance in 14 kilogauss fields, and the other to describe the high-frequency version for ^{13}C(68MHz) - ^{1}H(270 MHz) experiments in a 63-kilogauss superconducting magnet.

A rather standard system of equations needs to be solved to estimate the component values for a particular case. Tuning and impedance-matching conditions

on the low-frequency circuit require, respectively:

$$\frac{1}{\omega_1 C_1} + \frac{1}{\omega_1 C_2} \sim \omega_1 L \tag{1}$$

$$\frac{1}{\omega_1 C_2} \sim \sqrt{R\, R_{o1}} \tag{2}$$

and similar conditions for the high-frequency circuit require:

$$\frac{1}{\omega_h C_3} + \frac{1}{\omega_h C_4} \sim \omega_h L \tag{3}$$

$$\frac{1}{\omega_h C_4} \sim \sqrt{R\, R_{oh}} \tag{4}$$

ω_1 and ω_h are the low and high frequencies in radians per second; R_{o1} and R_{oh} are the desired input impedances; and R is the effective series resistance of the coil. These equations were obtained from an essentially zeroth order approximation that involves ignoring small residual effects of C_1 and C_2 on the high-frequency response and of C_3 and C_4 on the low-frequency response of the probe. As long as the inequalities

$$R_{oc}{}^2 \omega_h C_2 >> \omega_h L \tag{5}$$

$$C_1, C_2 >> C_3 \tag{6}$$

(where R_{oc} is the coaxial cable characteristic impedance)

are maintained, this appears to be an adequate description, particularly since one must expect that the effective, in circuit, values will be affected (strongly at high frequencies) by the geometrical configuration of the probe, and thus the final values of all components must be empirically adjusted[18]. A proper choice of coil inductance, L, allows one to maintain inequalities[5,6]

as long as the two frequencies are sufficiently different. The low-frequency impedance matching capacitor, C_2, and the high-frequency impedance matching capacitor, C_4, are shown as fixed capacitors since impedance matching is not so critical as to require continuously adjustable capacitors at those points, and the practice was to add in parallel small fixed ceramic capacitors[19] to arrive within a few percent of the desired impedance. C_1 served as the low-frequency tuning capacitor while C_3 maintained the high-frequency tuning condition, and although both capacitors affect the tuning of both high and low frequency resonance, the large difference in the size of the capacitors $C_1/C_3 \sim \omega_h^2/\omega_l^2$ allowed nearly independent tuning. Point B is the high-impedance (high voltage) point for the higher frequency, while point D is the high-impedance point for the lower frequency, and, consequently, both capacitors C_1 and C_3 must be able to withstand the several kilovolts present at 100 watts of applied rf power.

A. Low-Frequency Version

For the situation where the probe was tuned for $\frac{\omega_l}{2\pi}$ = 14.2 MHz and $\frac{\omega_h}{2\pi}$ = 56.4 MHz and with R_{oh} = 200 Ω and R_{ol} = 50 Ω, we obtained a circuit with Q_h = 80, and Q_l = 60 when we used a solenoidal sample coil 1.5 cm long and 6 mm in diameter consisting of 14 turns of flattened #20 copper wire (measured inductance of 0.36 μH). The nominal (low-frequency) values of the capacitors used were: C_1 = 230 pf, C_2 = 820 pf, C_3 = 28 pf, and C_4 = 94 pf. The actual effective, in circuit, values of these capacitive elements differed substantially, particularly for the larger values of capacitance, from the nominal values as can be seen in comparing the reported values with the results of Equations 1-4.

The coil was designed to both furnish the desired inductance, L, and an intense, uniform H_1 field (H_1 inhomogeneity was measured to be 0.3% over a 4 mm diameter spherical sample, and with 100 watts of input power on both high and low frequencies, H_1 field strengths of 50 gauss were obtainable).

This version of the probe was designed for operation within a 4.8 cm wide gap of a conventional electromagnet, and consequently, no severe space problems

were encountered, and it was possible, for example, to use a conventional variable vacuum capacitor as part of C_1. A simple variable ceramic trimmer in parallel with a fixed ceramic capacitor was used for C_3. Temperature regulation capability was obtained by encasing the sample coil in a glass dewar (unsilvered) and simply passing the coil leads through the dewar walls. In addition, the probe was designed for use with an already existing rotational device for use in single crystal studies.

It was found necessary to take care to remove all dielectric materials containing protons when the proton signal was to be observed. In particular, a teflon dielectric $\lambda/4$ cable was used in this case, and likewise when the fluorine signal was to be observed, no fluorine-containing material was allowed as a dielectric.

B. High-Frequency Version

Because of the inherent difficulty of working with the high rf frequency used in this version (270 MHz), special care had to be taken in the physical construction of the probe and its components to avoid additional and undesirable inductances and capacitances. The solenoidal sample coil was again constructed from flattened copper wire (#16 flattened to a width of 2 mm) which was wound into a 9-turn, 1.4 cm long coil of 6 mm diameter. The measured inductance of the coil was near 0.16 μH and stayed frequency independent to well beyond 270 MHz. The high-frequency tuning and impedance-matching capacitors C_3 and C_4 were combined into a single cylinderical unit which is illustrated in Figure 2. The capacitor C_3 was formed by the central copper rod (which is connected directly to the coil at point B) and the adjustable inner cylinder. This capacitor has a restricted, but usable tuning range of from 1.5 to 3.5 pf. The capacitance between the outer two cylinders is near

40 pf, and since the outer cylinder is grounded, it constitutes the main part of the matching capacitor, C_4. Final adjusting of C_4 was accomplished by adding small fixed ceramic capacitors[19] between point C and the outer cylinder. This geometrical configuration allowed effective shielding of the bulky C_3 capacitor and furnished a low inductance ground connection between the incoming cable shielding and the ground side of the coil L (the incoming cable was soldered to the bolt at point C and the ground to the outer cylinder at that point). In this geometry it was necessary to add 36 pf of additional capacitance between point C and the outer cylinder for a 50 ohm impedance match with the incoming 270 MHz signal. For capacitor C_1 a variable capacitor identical in construction to that used for the C_3 part of the cylinderical unit illustrated in Figure 2,was used with additional fixed ceramic[19] capacitors in parallel to give a total capacitance of 32 pf. The $\lambda/4$ cable was a teflon-dielectric coaxial cable. The low-frequency matching capacitor, C_2, was large, 350 pf, and care had to be taken in its placement in order to maintain its value because even short leads could add sufficient inductance to radically alter its impedance. The exact length of the co-axial cable was determined experimentally such that the connection of the cable did not change the resonance frequency of the 270 MHz portion of the probe. With the $\lambda/4$ cable disconnected the Q of the 270 MHz resonant circuit was 300, and upon connection of the $\lambda/4$ cable, this figure dropped to 150. The Q of the 67.9 MHz portion was measured to be near 80, and no measurable power loss could be attributed to the $\lambda/4$ cable at this frequency.

The application of 330 watts of 270 MHz power was required to produce H_1 field strengths of 33 gauss, indicating some additional loss mechanism still unaccounted for in comparison to the low-frequency version. It was found necessary to use three ceramic capacitors[19] in series for the padding capacitor in parallel with the adjustable portion of C_1 since the application of 300 watts was sufficient to cause arcing across a single capacitor in this position.

III. Operational Characteristics

The actual operational configuration for the probe is illustrated in Figure 1. A power-activated diode (PAD) switch[20] was used to couple the transmitter and receiver to the probe circuit for the lower frequencies, and a $\lambda/4$ arrangement[8,16] was used for coupling at the higher frequency. Commercially available filters[21] were used at the probe inputs as illustrated in Figure 1. A wideband receiver (5-300 MHz), which has been previously described[22], was used for observing both frequencies by simply connecting the appropriate signal line to the receiver. The ability to use the same wideband receiver for both high and low frequency signals emphasizes the frequency isolation obtained with the combination of probe and commercial filters.

The probe was operated in two modes. In one case it was necessary to observe one frequency in the midst of a complex pulse cycle where, during a window of a few microseconds, no rf was being applied at either frequency. In this case the commercial filters were not used since they hindered recovery times. A 100-watt signal applied to either input of the probe resulted in a 10-15 volt peak-to-peak leakage signal at the opposite input, and this was

further reduced to less than one volt by the time it arrived at the receiver. The receiver was designed to handle volt-level transients[22], and signals could be observed, for example, from either protons or carbon-13 in the normal 4 microsecond sampling window of the eight-pulse cycle with a cycle time of 48 microseconds. In the second mode, it was necessary to observe one signal while simultaneously applying high rf power to the probe at the second frequency. The use of both of the commercial filters was necessary in this case in order to: (a) protect the receiver from overloading due to the high power rf signal at the second frequency, and (b) prevent the high-power input signal from containing any rf component at the detection frequency (once a signal of this sort reached the probe, it could not be removed by any filtering without also filtering out the NMR signal to be observed).

An example of the performance of the probe in this second mode is illustrated in Figure 3, which is an oscilloscope photograph of the ^{207}Pb NMR signal observed in PbF_2, with (bottom) and without (top) decoupling the ^{19}F. In the upper trace no fluorine decoupling power has been applied and the ^{207}Pb signal decays too rapidly (due to heteronuclear dipolar interactions) to be observed on this timescale (5 msec total scan), while in the lower trace fluorine decoupling power has been applied and the ^{207}Pb signal is clearly visible. One notes that the presence of the high-power level of fluorine irradiation has not produced any noticeable increase in the noise observed at the ^{207}Pb frequency. Other examples of the quality of data obtained can be found in recently published papers[2,3,4].

Acknowledgment

This work was supported by the Office of Naval Research. In addition, we would like to gratefully acknowledge funds used for construction of the NMR spectrometers from the National Science Foundation, the Alfred P. Sloan Foundation, the Camille and Henry Dreyfus Foundation, the Ford Motor Company, and the Mobil Oil Corporation. Discussions with John Yehle and Dr. J. E. Piott are gratefully acknowledged.

References

† On leave from the Weismann Institute of Science, Rehovot, Israel.

1. M. E. Stoll, W-K. Rhim, and R. W. Vaughan, J. Chem. Phys. 64, 4808 (1976).
2. M. E. Stoll, A. J. Vega, and R. W. Vaughan, J. Chem. Phys. 65, 4093 (1976).
3. M. E. Stoll, A. J. Vega, and R. W. Vaughan, Proceedings of the XIXth Congress Ampere, Heidelberg, Germany, 1976. In press.
4. M. E. Stoll, A. J. Vega, and R. W. Vaughan, submitted for publication.
5. W. G. Clark, Rev. Sci. Instrum. 35, 316 (1964).
6. W. G. Clark and J. A. McNeil, Rev. Sci. Instrum. 44, 844 (1973).
7. I. J. Lowe and M. Engelsberg, Rev. Sci. Instrum. 45, 631 (1974).
8. I. J. Lowe and C. E. Tarr, J. Phys. E1, 320 (1968).
9. V. R. Cross, R. K. Hester, and J. S. Waugh, Rev. Sci. Instrum. 47, 1486 (1976).
10. J. D. Ellett, M. G. Gibby, U. Haeberlen, L. M. Huber, M. Mehring, A. Pines, and J. S. Waugh, Advances in Magnetic Resonance (Ed.: J. S. Waugh). Vol. V, p. 117, Academic Press, New York, 1971.
11. K. W. Gray, W. N. Hardy, and J. D. Noble, Rev. Sci. Instrum. 37, 631 (1966).
12. R. A. McKay and D. E. Woessner, J. Sci. Instrum. 43, 838 (1966).
13. N. Trappeniers, N. J. Gerritsma, P. H. Oosting, Physica 30, 997 (1964).
14. M. Mansfield, J. G. Powles, J. Sci. Instrum. 40, 232 (1963).
15. I. J. Lowe and D. E. Barnaal, Rev. Sci. Instrum. 34, 143 (1963).
16. U. Haeberlen, Ph.D. Thesis, Tech. Hochschule, Stuttgart, 1967.
17. The use of a $\lambda/4$ cable for frequency isolation within the probe was initially suggested to us by Prof. M. Mehring (unpublished material).

18. Empirical characterization of circuit behavior was accomplished with a Hewlett-Packard impedance meter below 100 MHz and a vector voltmeter (Model 8405A) above 100 MHz.

19. American Technical Ceramics, 1 Norden Lane, Huntington Station, New York, high voltage ATC Model B capacitors.

20. J. E. Piott, D. L. Husa, and M. Lipsicas, submitted for publication.

21. Cir-Q-tel Inc., 10504 Wheatley Street, Kensington, Maryland 20795.

22. R. W. Vaughan, D. D. Elleman, L. M. Stacey, W.-K. Rhim, and J. W. Lee, Rev. Sci. Instrum. 43, 1356 (1972).

Figure Captions

Figure 1: (A) Schematic diagram of double resonance probe. The high-frequency connection is at point C , while the low-frequency connection is at point A . Inductor, L, represents the sample coil, R represents losses in the coil and remaining circuit, and ℓ is the length ($\lambda/4$ at the high frequency) of a piece of coaxial cable.

(B) Connection of probe to receiver and transmitter. The optional filters (F_l and F_h) are shown with dotted outline, and the connection of either frequency to the broadband receiver is made through a conventional $\lambda/4$ arrangement or a PAD switch (P).

Figure 2: Cross section of unit which comprises capacitors C_3 and C_4 in higher frequency version of probe. Points B and C correspond to those in Figure 1. Respective diameters are: a = 0.32 cm, b = 1.11 cm, c = 1.59 cm, d = 2.22 cm, e = 2.38 cm, and f = 0.64 cm. A similarly constructed unit, without the outer metal ground (d and e), served as the adjustable portion of capacitor C_1.

Figure 3: Free-induction decay of ^{207}Pb in solid PbF_2 without (top trace) and with (bottom trace) ^{19}F decoupling. The horizontal axis is 5 msec fullscale, and no ^{207}Pb NMR signal is observed in the top trace on this timescale due to heteronuclear dipolar broadening, while the decoupled ^{207}Pb signal is apparent in the lower trace. Comparison of the two traces shows no observable increase in the noise level on the 12.5 MHz channel (^{207}Pb) when high power is applied to the 56.4 MHz channel (^{19}F).

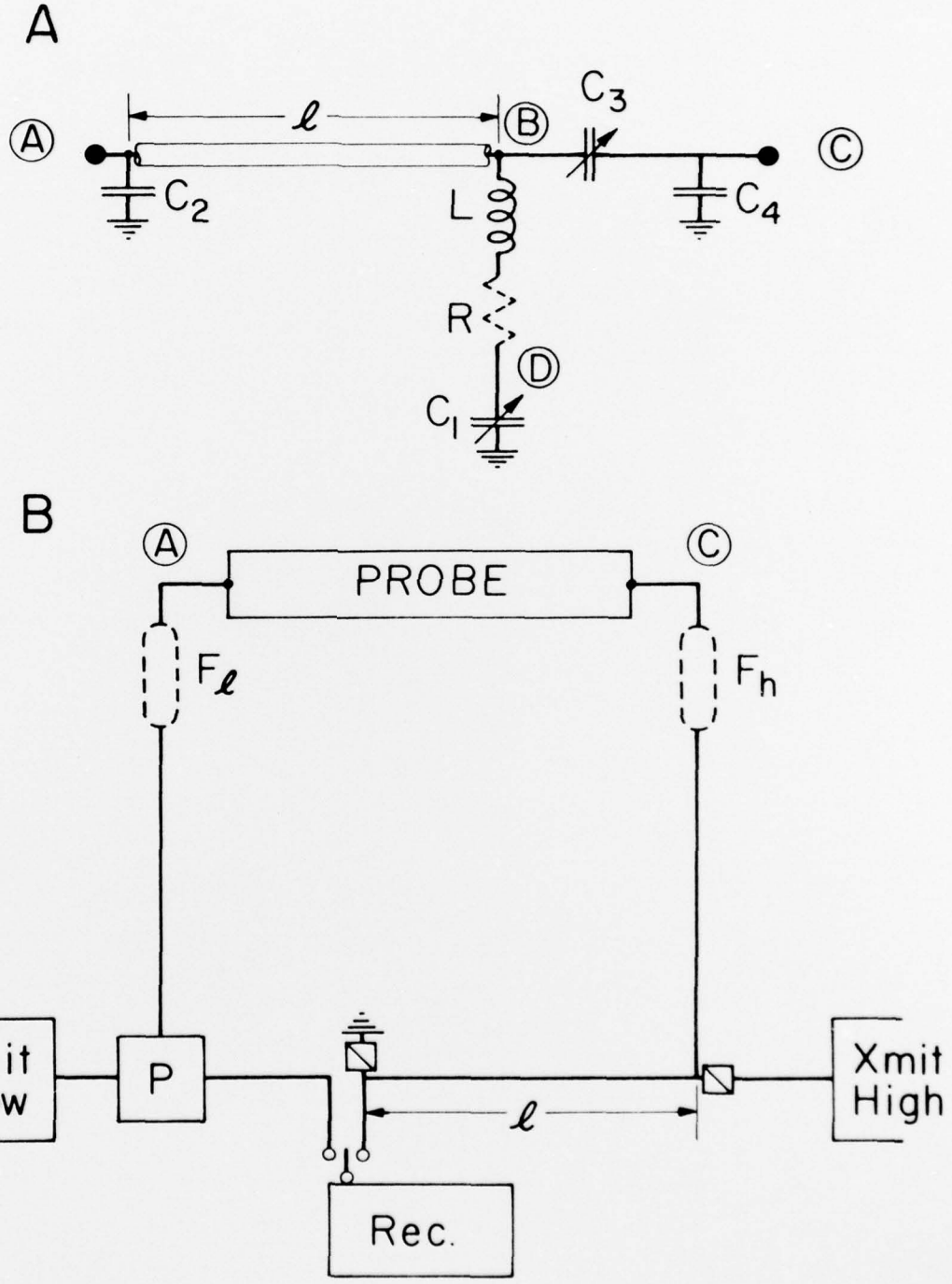

Figure 1

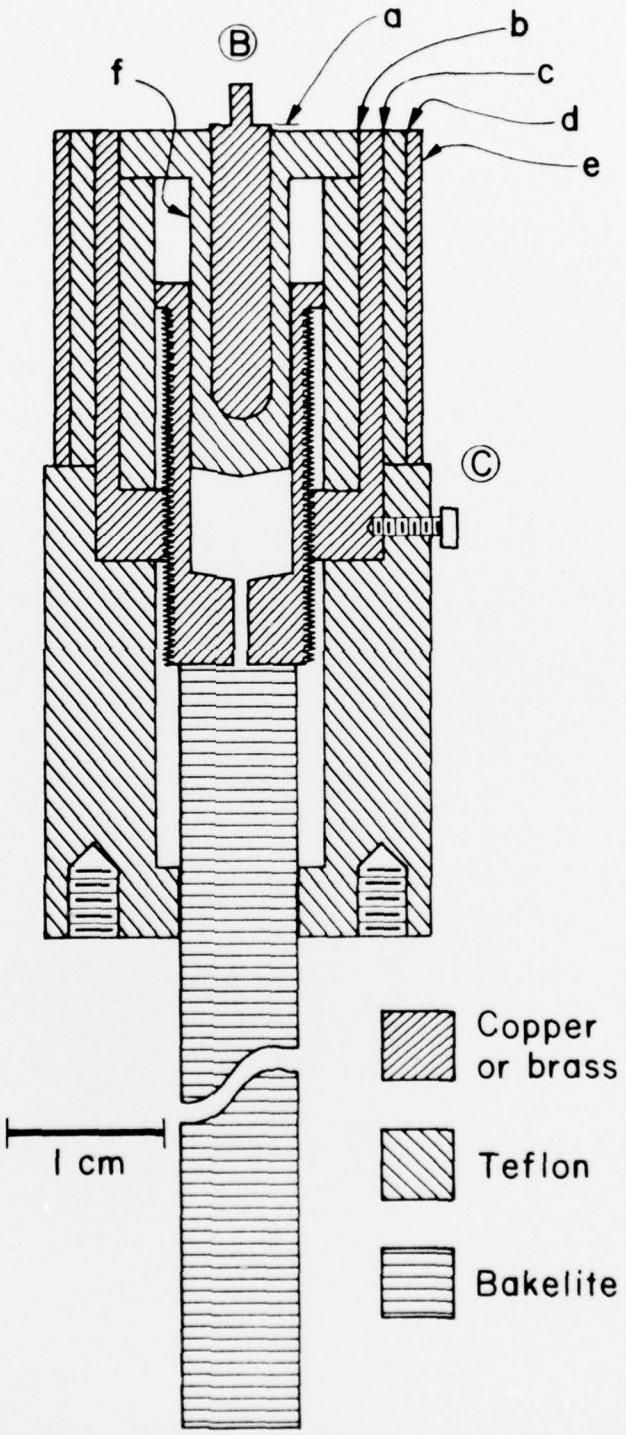

Figure 2

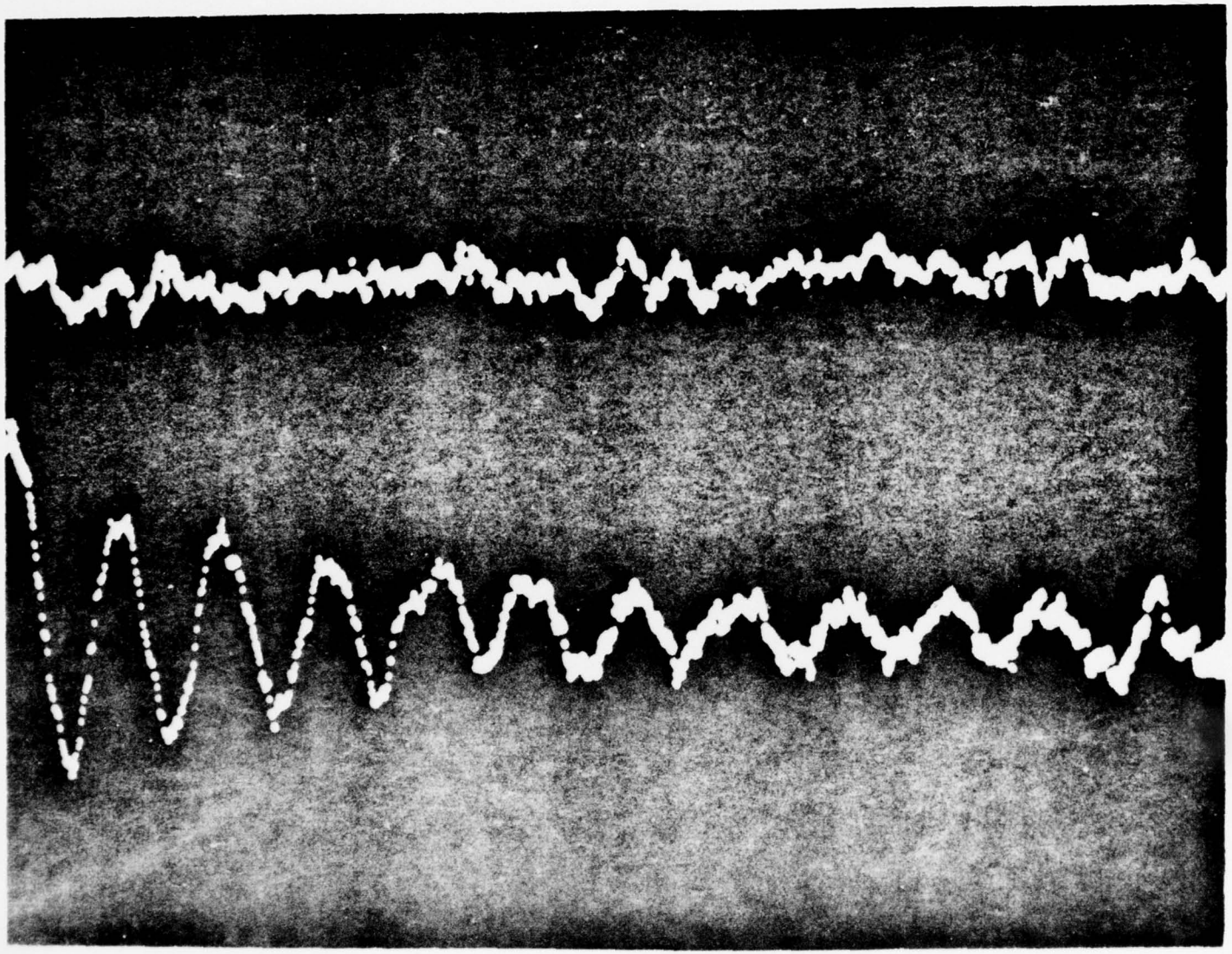

Figure 3

TECHNICAL REPORT DISTRIBUTION LIST

	No. Copies
Office of Naval Research Arlington, Virginia 22217 Attn: Code 472	2
ONR Branch Office 536 S. Clark Street Chicago, Illinois 60605 Attn: Dr. George Sandoz	1
ONR Branch Office 207 West 24th Street New York, New York 10011 Attn: Scientific Dept.	1
ONR Branch Office 1030 East Green Street Pasadena, California 91106 Attn: Dr. R. J. Marcus	1
ONR Branch Office 760 Market Street, Rm. 447 San Francisco, California 94102 Attn: Dr. P. A. Miller	1
ONR Branch Office 495 Summer Street Boston, Massachusetts 02210 Attn: Dr. L. H. Peebles	1
Director, Naval Research Laboratory Washington, D. C. 20390 Attn: Library, Code 2029 (ONRL) Technical Info. Div. Code 6100, 6170	6 1 1
The Asst. Secretary of the Navy (R&D) Department of the Navy Room 4E736, Pentagon Washington, D. C. 20350	1
Naval Surface Weapons Center White Oak Silver Spring, Maryland 20910 Attn: Code 230	1
Dr. P. R. Antoniewicz University of Texas Department of Physics Austin, Texas 78712	1
Dr. L. N. Jarvis Surface Chemistry Division 4555 Overlook Avenue, S. W. Washington, D. C. 20375	1

	No. Copies
Commander, Naval Air Systems Command Department of the Navy Washington, D. C. 20360 Attn: Code 310C (H. Rosenwasser)	1
Defense Documentation Center Building 5, Cameron Station Alexandria, Virginia 22314	12
U. S. Army Research Office P. O. Box 12211 Research Triangle Park, North Carolina 27709 Attn: CRD-AA-IP	1
U. S. Naval Oceanographic Office Library, Code 1640 Suitland, Maryland 20390	1
Naval Ship Research & Development Center Annapolis Division Annapolis, Maryland 21402 Attn: Dr. Allan Evans, Code 2833	1
Commander Naval Undersea Research & Development Center San Diego, California 92132 Attn: Technical Library, Code 133	1
Naval Weapons Center China Lake, California 93555 Attn: Head, Chemistry Division	1
Naval Civil Engineering Laboratory Port Hueneme, California 93041 Attn: Mr. W. S. Haynes	1
Professor O. Heinz Department of Physics & Chemistry Naval Postgraduate School Monterey, California 93940	1
Dr. A. L. Slafkosky Scientific Advisor Commandant of the Marine Corps (Code RD-1) Washington, D. C. 20380	1
Dr. W. M. Risen, Jr. Brown University Department of Chemistry Providence, Rhode Island 02912	1

MAILING LIST

Dr. John B. Hudson
Rennselaer Polytechnic Institute
Materials Engineering Division
Troy, New York 12191

Dr. K. H. Johnson
Massachusetts Institute of Technology
Dept of Metallurgy and Materials Science
Cambridge, Massachusetts 02139

Dr. W. D. McCormick
Dept of Physics
University of Texas
Austin, Texas 78712

Dr. G. A. Somorjai
Dept of Chemistry
University of California/Berkeley
Berkeley, California 94720

Dr. Robert W. Vaughan
California Institute of Technology
Division of Chemistry and Chemical Engineering
Pasadena, California 91125

Dr. David A. Vroom
INTELCOM RAD TECH
P.O. Box 80817
San Diego, California 92138

Dr. J. Bruce Wagner, Jr.
Northwestern University
Evanston, Illinois 60201

Dr. J. M. White
Dept of Chemistry
University of Texas
Austin, Texas 78712

Dr. John T. Yates, Jr.
U.S. Dept of Commerce
National Bureau of Standards
Surface Chemistry Section
Washington, D.C. 20234

Dr. Lennard Wharton
Dept of Chemistry
James Franck Institute
5640 Ellis Avenue
Chicago, Illinois 60637

Dr. J. E. Demuth
International Business Machines Corp.
Thomas J. Watson Research Center
P.O. Box 218
Yorktown Heights, New York 10598

Dr. C. P. Flynn
University of Illinois
Dept of Physics
Urbana, Illinois 61801

Dr. W. Kohn
Department of Physics
University of California (San Diego)
La Jolla, California 92037

Dr. T. E. Madey
National Bureau of Standards
Surface Processes and Catalysis Section
Washington, D.C. 20234

Dr. R. L. Park
Director, Center of Materials Research
University of Maryland
College Park, Maryland 20742

Dr. W. T. Peria
Electrical Engineering Dept
University of Minnesota
Minneapolis, Minnesota 55455

Dr. Narkis Tzoar
City University of New York
Convent Avenue at 138th Street
New York, New York 10031

Dr. R. F. Wallis
Depatment of Physics
University of California/Irvine
Irgine, California 92664

Dr. Chia-wei Woo
Northwestern University
Dept of Physics
Evanston, Illinois 60201

Dr. Mark S. Wrighton
Dept of Chemistry
MIT, Rm 6-335
Cambridge, Massachusetts 02139